의학박사 학위논문

Liposomal delivery of mesoporous silica-coated iron oxide magnetic nanoparticles for theranostic application

치료진단적 적용을 위한 다공성 실리카 코팅
산화철 자성 나노파티클의 리포좀을 이용한 전달

2017년 2월

서울대학교 의과대학원

의학과 핵의학전공

장 수 진

Liposomal delivery of mesoporous silica-coated iron oxide magnetic nanoparticles for theranostic application

지도 교수 이 동 수

이 논문을 의학박사 학위논문으로 제출함
2017년 12월

서울대학교 의과대학원
의학과 핵의학전공
장 수 진

장수진의 의학박사 학위논문을 인준함
2017년 1월

위 원 장 정 재 민 (인)

부위원장 이 동 수 (인)

위 원 최 준 영 (인)

위 원 이 윤 상 (인)

위 원 황 도 원 (인)

논 문 초 록

치료진단적 적용을 위한 다공성 실리카 코팅 산화철 자성 나노파티클의 리포좀 전달

암조직의 영상화가 가능하면서 동시에 암세포에 치료제를 효과적으로 전달할 수 있는 나노입자의 개발을 위해 다양하고 많은 연구들이 시도되었으나 나노입자 자체의 독성이 문제가 되거나 충분한 양의 치료제를 담을 수 있는 나노운반체를 만들기 어렵다는 점 때문에 실제 임상에서의 암환자 치료에 도입되기 어려웠다. 이 연구에서는 이러한 제한점을 극복하기 위하여 산화철을 일련의 화학반응을 이용하여 다공성 실리카로 표면 처리한 자성 나노입자(MNP@*m*SiO_2)를 개발하였으며 그 자성과 물리적 성상이 안정적으로 유지됨을 확인하였다. 표면처리를 하지 않은 산화철 나노입자가 산성 용액에 노출 될 경우 해체되는 반면 MNP@mSiO_2는 안정성을 유지하였고 그 자성(r_2=270 $mM^{-1}\cdot S^{-1}$)은 무정형 실리카로 처리한 산화철 나노입자(70 $mM^{-1}\cdot S^{-1}$)에 비해 월등히 높으면서 산화철 나노입자 본연의 자성(286 $mM^{-1}\cdot S^{-1}$)과 유사하게 유지되었다. 그러나 다공성 실리카 조성은 버퍼용액 내 안정성에 취약하여 생물학적 활용에 부적합하였으므로 리포좀 복합체를 이용하여 안정성을 확보하는 동시에 기존의 나노입자보다 많은 양의 치료제를 담을 수 있도록 하였다(MagLipo).

Cryo-TEM 분석 결과 약 6-8개의 MNP@mSiO$_2$ 입자가 하나의 리포좀 입자 내에 봉입되었으며 MNP@*m*SiO$_2$와 달리 MagLipo는 인산염 버퍼용액에서 장시간 안정성을 유지하였다. 이렇게 구성된 MagLipo 표면에 EGFR 항체를 결합(EGFR-MagLipo)하여 췌장암 세포주의 선택적 검출을 시도하였고 췌장암세포에서 이상 증폭되는 Plk1 단백질 합성을 방해하는 siRNA를 항암제인 doxorubicin과 함께 탑재하여 선택적으로 전달하고 암세포 특이적 환경에 반응하여 치료제를 방출하도록 기획 하였다. 최종적으로 구성된, T_2 증강 영상이 가능함과 동시에 암세포의 선택적 검출 및 치료를 목적으로 하는, 치료진단용 나노파티클의 검출 효율 및 치료 효과를 췌장암 세포주 실험으로 확인하였다. 암세포 진입 후 리소좀 내 특이적 환경을 반영하는 pH 4.7의 용액에서 doxorubicin을 탑재한 MagLipo는 30분 이내에 약제의 40%를 방출하였다. *T_2-w* phantom 실험에서 MagLipo를 처리한 췌장암 세포와 대조군 세포는 유사한 신호강도를 보였으나 EGFR-MagLipo를 처리한 췌장암 세포의 경우 유의한 T2 신호의 감소(≈80%)를 보였다. 항암제와 치료용 siRNA를 모두 탑재한 MagLipo를 처리한 경우 각각을 따로 처리한 경우와 비교하여 치료의 상승효과가 있음을 확인하였다. 이상의 결과를 바탕으로 MagLipo는 다기능의 나노물질로써 향후 암의 표적치료와 영상진단을 동시에 수행할 수 있는 nanovehicle의 개발에 기여할 것으로 기대된다.

주요어 : 자성 나노입자, 리포좀, 다공성 실리카, 치료진단 나노입자, pH-감응성 약제전달
학 번 : 2008-30538

Table of contents

List of figures

Introduction

Nanoparticles for the biomedical applications have been studied in an effort to find the most efficient way to deliver the drug and/or gene for therapeutic purposes (*1-4*). Besides for the therapeutic applications, several nanomedicine formulations combining disease diagnosis and therapy have been developed, and these 'theranostic' nanomaterials are considered as highly suitable systems for monitoring drug delivery, drug release, and drug efficacy (*5*). Especially, metal nanoparticles are suggested as attractive theranostic agents for cancer owing to its inherent physicochemical properties providing both carriers for the various therapeutic moieties and tools for the medical imaging. Various methods to fabricate nanoparticles for the establishment of multifunctional and biocompatible theranostic systems have been introduced (*6*).

Among various metal nanoparticles, quantum dot or iron oxide nanoparticles possess unique optical or magnetic properties and have received attention for decades as appealing candidate materials for imaging diagnosis (*7-9*). However, particles consist of heavy metal ions such as Cd, or Mn presented potential toxicological issues (*10,11*). Ions from these particles tend to be released in acidic conditions, which cause serious toxicity problems. To overcome the decomposition of the metal ions, researchers have utilized the silica shell coating, which has a relatively low toxicity and high acid resistance, onto the metal oxide nanoparticles (*12-14*).

In the group of nanoparticles with various inorganic compositions, iron oxide-based nanoparticles are in unique position since considerable store of experience and knowledge regarding it has been accumulated for decades (*15*) and

many studies have reported iron oxide nanoparticles are biocompatible materials with negligible toxicity (*16,17*). In biomedical field, iron oxide magnetic nanoparticles (MNPs) are utilized for various applications such as magnetic resonance imaging (MRI), drug delivery, controlled drug release, cell labelling, cell separation, and nanoscale biosensor (*18*). MNPs with a higher relaxivity are preferred in order to increase detection sensitivity in MR-based imaging or sensing (*19,20*). To increase transverse relaxivity (r_2), size and chemical composition of the particles need to be tuned (*21-23*). The value of r_2 is proportional to the size (d) and saturated magnetism (*Ms*, $r_2 \propto d^2 \cdot M_s^2$) (*24,25*). Since iron oxide MNPs are sensitive to the acid corrosion, to improve stability and safety of the metal oxide, silica shell coatings have been most commonly used for the preparation of functionalized iron oxide nanoparticles. However, the shell was spiked with a lowered value of r_2 due to a decrease in the number of water molecules adjacent to the MNP core (*26*).

In this study, to solve the problems of stability, safety, and efficiency of magnetic nanoparticles, the mesoporous silica (mSiO$_2$) shell was coated onto a magnetic iron oxide nanoparticle (MNP@mSiO$_2$). Mesoporous silica, having large surface area, good biocompatibility, and chemical and thermal stability, provides suitable conditions for the biomedical applications of nanocarriers (*27*). Also, the shell possesses a sufficient amount of water molecules inside the pores near the core particles to minimize the decrease in magnetic relaxivity (*28*). Furthermore, the pore structures can provide roomy space for the incorporation of therapeutic load. We chose doxorubicin (Dox), an anticancer drug, to be packaged in the nanoparticles. Dox, one of the anthracyclines, exerts its anticancer effects by intercalating into the double-stranded DNA, inhibiting topoisomerase II enzyme,

and forming free radicals damaging cells. It is well known as a potent anticancer drug against many types of cancer (*29*). Since mitochondrial membranes are especially sensitive to the oxidative damage by Dox, high cardiotoxicity is most important clinical consideration in chemotherapeutic regimens with Dox because heart muscles are rich in mitochondria (*30*). As an effective chemotherapeutic drug with dangerous cardiotoxicity, like a double edged sword, Dox is considered as an attractive candidate for the liposomal delivery (*31*). Also, its intrinsic fluorescence allows intracellular localization of drug using microscopic technique (*32*). Together with the chemotherapeutic agent (Dox), we adopted RNA interference-mediated silencing of proto-oncogene (Polo-like kinase 1, Plk1) to promote chemosensitivity of cancer cell to Dox (*33*) and synergistic therapeutic effect. Plk1 is overexpressed in a broad range of human cancers and is associated with poor prognosis (*34-37*). Several preclinical therapeutic attempts targeting Plk1 showed promising results (*38-40*) and a nanoparticle formulation of *si*RNA for inhibition of Plk1 is in a clinical trial study for the treatment of advanced solid tumors (*41*). Consequently, both hydrophilic drug (Dox) and the *si*RNA for the silencing of Plk1, could be incorporated into the mesoporous silica shell of MNP@*m*SiO_2 for the material to possess therapeutic ability. To improve their bio-applicability, liposomal complex systems were combined with the MNP@*m*SiO_2 particles (MagLipo). Even though nanoparticles are expected to accumulate in the tumors with higher concentration than the normal tissue, as explained with the EPR (enhanced permeability and retention) effect (*42*), intratumoral distribution of nanoparticles could be insufficient due to various factors such as disordered tumor vasculature and extensive tumor stroma. Therefore, adoption of recognition moiety for the cellular surface target that is upregulated in pancreatic cancer cells, but is poorly or not

expressed in normal tissues is recommended (*43*). In this way, active targeting along with passive targeting can potentially confer higher detection sensitivity, advanced delivery efficacy, and minimal off-target toxicity on the nanoparticles (*44*). Cancer-specific antibodies for the epidermal growth factor receptor (EGFR-Ab) were anchored onto the MagLipo particles (EGFR-MagLipo) through bio-conjugation chemistry to render specific targeting, based on that the EGFR is overexpressed in pancreas cancer and is a good subject for the molecular targeted therapy (*45*). Above mentioned processes and results of this study is well documented in the recently published article (*46*).

In summary, an attempt has been made to construct a novel theranostic nanoparticle system combining magnetic property for MR imaging and drug delivery system for cancer therapy, which can specifically target cancer cells and release drugs in stimulus-sensitive manner. The physicochemical properties of current nanoparticle (MagLipo), as a carrier system and imaging modality, were characterized. Then, the cellular uptake, intracellular localization, pH-sensitive drug release, anticancer activity, and synergistic therapeutic efficacy of simultaneous delivery of drug and siRNA were determined in human pancreas cancer cell line.

Materials and methods

Chemicals

Tris (acetylacetonate) iron (III) [$Fe(acac)_3$, 99.9%], iron (II) acetylacetonate [$Fe(acac)_2$, 99.95%], 1,2-hexadecanol (90%), oleic acid (OA, 99%), oleylamine (OY, 70%), 1-octadecene (ODE, 95%), chloroform (99%), dimethyl sulfoxide (99.9%), and *N*-hydroxysulfosuccinimide sodium salt (98.5%) were purchased from Sigma-Aldrich, and used without further modifications. The lipid chemicals were purchased from Avanti Polar Lipids Inc. (Alabaster, AL, USA). Isopropanol (99.5%), hexane (98.5%), ethanol (99.5%), and $NaHCO_3$ were purchased from Fisher Scientific, Korea Ltd., and used without further purification.

Preparation of 16-nm sized iron oxide magnetic nanoparticles (MNPs) and MNP@SiO_2 particles with Dox

We first synthesized 10 nm sized MNPs as seeds for subsequent particle growth. $Fe(acac)_3$ (4 mmoL, 1.4 g), $Fe(acac)_2$ (2 mmoL, 0.5 g), 1,2-hexadecanediol (10 mmoL, 2.9 g), OA (6 mmoL, 1.9 mL), OY (6 mmoL, 2.8 mL) and ODE (20 mL) were mixed by stirring under N_2 flow for 1 hr. The mixture was heated and kept at 200°C for 2 hr. The temperature was then quickly raised to 280°C to initiate particle formation. After reflux, the mixture was cooled to room temperature and isopropanol (4 mL) was added. MNPs were collected by centrifugation (7000 rpm, 15 min) and the precipitates were re-dispersed in hexane. To make larger MNPs

from the seed particles, 10 nm MNPs (100 mg) were dissolved in hexane (10 mL) together with the same amounts of metal acetylacetonates, 1,2-hexadecanediol, OA, OY and ODE as described above. Under N_2 flow, the mixture was heated and kept at 100°C for 1 hr. The temperature was then elevated to 200°C and maintained for two hours. Finally, the mixture was heated again to 300°C and refluxed for 2 hr before being cooled down to room temperature. The 12 nm MNPs were collected by the same washing and isolation procedures aforementioned. In a similar manner, 16 nm MNPs were prepared using these 12 nm particles as seeds. To determine the magnetic relaxivity of the MNP, the particles were dispersed in H_2O after being treated with CTAB chemicals. TD-NMR (Minispec mq20, 0.47 T, Bruker, Billerica, MA, USA) was used to determine the relaxivity of the particles (r_2).

To generate water-soluble MNP, at first 600 μL particle solution in 2 mg/mL chloroform ($CHCl_3$) and 0.05 mM hexadecyltrimethylammonium bromide (CTAB) 5 mL were mixed and vigorously stirred for 1 hr in a 2-neck round bottom flask. And then the temperature was increased to 60°C for removing organic solvent. After 20 min, added 25 mL distilled water and 1.8 mL NaOH (2 N) at 70°C. Stirred ethyl acetate (EA) 1.8 mL into this mixture and slowly dropped tetraethylorthosilicate (TEOS) 0.3 mL for 6 hr. After completion of reaction, the mixture was centrifuged for 20 min at 14,000 rpm and washed with ethanol and distilled water separately. To remove CTAB in the product completely, added HCl 0.05 mL solution and then vigorously stirred for 30 min. The schematic illustration of synthesis of MagLipo is presented in Figure 1A.

The morphological features, structure, composition, and magnetic properties of the resulting 80 nm iron oxide mesoporous silica-core-shell

nanoparticles (MNP@*m*SiO_2) were characterized using a transmission electron microscope (TEM; JEOL 2100, JEOL, Peabody, MA, USA), an X-ray powder diffractometer (XRD; RU300, Rigaku, Kyoto, Japan), and a vibrating sample magnetometer (VSM), respectively. To confirm the resistance of the meso-porous silica shell to acid corrosion, the MNP and MNP@*m*SiO_2 particles were dispersed in a 1 N HCl solution. To load therapeutic drug (Dox), 0.127 μmol of Dox was dissolved in 2 mL MNP@*m*SiO_2 (2 mg) aqueous solution and then homogeneously stirred for 2 hr at 60°C. The Dox loaded particle solution was centrifuged to remove unloaded Dox (13,000 rpm, 10 min) and repeated washing step with cleaned H_2O.

Drug loading capacity (HPLC analysis)

To evaluate the loading capacity of Dox in MNP@*m*SiO_2 particles, the supernatant solution of excess Dox after centrifugation was analyzed quantitatively by HPLC (hydrosphere C18 column: 4.6 x 50 mm, 3 μm, Agilent 1200, Santa Clara, CA, USA). The eluent solution (0.01% perfluorobutyric acid, 0.1% isopropanol in water) was utilized with optimized rate (1.0 mL/min) and Dox intensity was determined by equipped fluorescence spectroscopy (ex. 485 nm and em. 590 nm).

Preparation of liposome encapsulated MNP@*m*SiO_2 (MagLipo) particles

1,2-Dipalmitoyl-sn-glycero-3-phosphatidylcholine (DPPC, 20 μmol, 15.4 mg), diacetyl phosphate (DCP, 1.8 μmol, 1.0 mg), 1,2-distearoyl-sn-phosphoethanolamine-*N*-[PDP(polyethylene glycol)-2000] (DSPE-PEG-PDP, 5.0 mg), and cholesterol (3.48 mg) were dissolved in 5 mL chloroform (99.9%, Sigma-Aldrich, St. Louis, MO, USA). The mixed solution was allowed to evaporate for 5 min at room temperature and was then freeze-dried for 24 h at -45°C to induce the formation of a phospholipid film. Subsequently, 3 mL MNP@*m*SiO_2 (4 mM Fe) in 30 mM NH_4HCO_3 solution underwent sonication for 5 min at 60°C. The solution was subjected to a freeze-thaw cycle five times, using liquid nitrogen and a water bath. The prepared Lipo dispersion solution was extruded through a 200 nm filter at 60°C (mini-extruder, Avanti polar lipids). The excess organic chemicals were continually removed by centrifugation (5 min at 13,000 rpm) and washing with H_2O. The size distribution of the prepared nanoparticles (MNP, MNP@*m*SiO_2 and MagLipo) was measured by dynamic light scattering (DLS) analysis. The solubility of MNP@*m*SiO_2 and MagLipo was tested in DW and in PBS respectively.

Encapsulation of therapeutic gene into the MagLipo

For the synergistic therapeutic effect, the *si*RNA for Plk1 (*si*Plk1) was loaded into the MagLipo particles with pH-sensitive NH_4HCO_3 gradient method (*47,48*). To prepare Protamine (PA, 7.5 kDa) and *si*Plk1 complex, the *si*Plk1 gene (50 μM) and different concentration of PA solutions (0.3 ~ 12 μM) were incubated for 1 hr at room temperature using a plate shaker. And the ratio of PA and *si*Plk1 concentration was determined to be 12: 5 X 10^{-6} M by electrophoresis. To load

*si*Plk into the liposome, the fresh PA and *si*Plk1 complex solution was homogenized into MagLipo films (21 mg, 2 mL) for 5 min at room temperature, using electrophoresis. The MagLipo particles harboring *si*Plk1-PA were washed twice with centrifugation (5 min at 13,000 rpm) to remove the unloaded gene complex and the loading capacity was then estimated with a UV-Vis spectrophotometer.

Antibody conjugated onto the MagLipo and toxicology study

Cancer-specific antibodies were anchored onto the MagLipo particles (EGFR-MagLipo) through bio-conjugation chemistry to render specific targeting. To conjugate cancer specific antibody (anti-EGFR, AbCAM), the amine terminated particles (0.05 mM) were dispersed in 2 mL phosphate-buffered saline (PBS) and then added with Sulfo-SMCC (5 mg) in order to make the maleimidide chemical functional group. The mixture was stirred for 2 hr at room temperature. The nanoparticle solution was precipitated down (13,000 rpm, 15 min) and washed three times with H_2O. On the other hand, we activated EGFR antibody with Traut's reagent for the thiolation of EGFR antibody according to Pierce protocol. Anti-EGFR antibody (0.2 mg) and cysteamine (2-MEA, 1 mg) were dissolved in 2 mL EDTA solution (10 mM, Sigma-Aldrich), followed by incubation in a shaking incubator for 1.5 hr at 37°C. The thiol-active antibody was purified with PD-10 desalting column (GE Healthcare Bio-Sciences, Little Chalfont, UK) and immediately combined with the maleimide terminated MagLipo (0.05 mL). The mixture was shaken for 6 hr at 4°C and subsequently purified through

centrifugation. The toxicological study of the MagLipo-based particles was conducted using fibroblast (293T, EGFR negative) and pancreatic cancer (BxPC3, EGFR positive) cell lines with increasing concentration of EGFR-targeting and bare MagLipo particles. The expression levels of EGFR in both cell lines were determined by western blotting.

T_2-*w* MR phantom study

To demonstrate the utility of MagLipo particles for magnetic resonance imaging (MRI), we used the particles to detect pancreatic cancer cells in T_2-w signal phantom studies that involved MRI instruments (Achieva 3.0 T, TR/TE: 3500/7 ms). 3 μM [Fe] concentration of the particles were incubated with EGFR-positive BxPC3 cells for 3 hr inside a 5% CO_2 incubator. Subsequently, the excess particles were removed by washing the cell culture with PBS, and the treated cells (1 x 10^6/dish) were detached by trypsinization and subsequently centrifuged at 3,000 rpm and subjected to T_2-*w* signal phantom studies using MRI. All T_2-*w* MR images were acquired on a 3.0-T clinical MR scanner (Achieva Release 3.2.1.0 version, Philips medical system, Netherland). T_2-*w* images were obtained with a TR 3.5 s, a TE 7 ms. Using a time domain-NMR magnetic relaxometer, cellular relaxivity of the EGFR-MagLipo-treated cell solution was evaluated to measure detection sensitivity. The change in T_2 (ΔT_2 %) was determined based on the decrease in the number of cells and by its sensitivity towards the cancer cells.

Delivery of therapeutic moieties

The confocal laser scanning microscope was used to monitor the location of the Dox in MagLipo during delivery by its inherent red fluorescence property. The cells were seeded onto coverslips placed in a six-well plate for overnight and then incubated with MagLipo particles harboring Dox for 3 hr in serum free media. Afterward, the cells on coverglass, PBS-washed 3 times, were stained with DAPI for 5 minute to localize nuclei, and then washed 3 times with PBS again. After fixation of cells with formaldehyde solution, the prepared slides were analysed by confocal laser scanning microscope (LSM700, Zeiss, Oberkochen, Germany). Intensity profiles of Dox and nucleus stained with DAPI directly after administration and 24 hr after administration were plotted to demonstrate the ability of Dox in MagLipo to penetrate the nucleus. The Plk1 expression level of various cells was also analysed using the quantitative polymerase chain reaction (PCR) analysis with RT-PCR kit from ThermoFisher scientific (Waltham, MA USA) according to the instruction from supplier.

Cell viability assay

A 3-(4,5-dimethylthiazol-2-yl)-2,5-diphenyltetrazolium (MTT) assay kit (Invitrogen) was used to evaluate cell viability in the presence of particles. 293T fibroblasts were cultured in Dulbecco's Modified Eagle Medium (DMEMH16, Gipco, Grand Island, New York, U.S.A.), supplemented with fetal bovine serum (FBS, 10%), penicillin and streptomycin (1%), L-glutamine (1%) and sodium bicarbonate (2%). BxPC3 pancreatic cancer cells were cultured in vendor-provided

media. Cells were maintained at 37°C in a humidified atmosphere containing 5% of CO_2. At confluence, the cells were washed, trypsinized, and resuspended in culture media. Cells were then seeded at a concentration of 5,000 cells/well in a 96-well tissue culture plate and allowed to grow overnight at 37°C under 5% CO_2. Aqueous particle solutions at different particle concentrations were added into the culture media, and the cells were allowed to grow for another 24 hr. For cell viability test, the culture media was replaced with MTT solution. After 3 hr of incubation at 37°C under 5% CO_2, MTT solubilization solution was added to dissolve the resulting formazan crystal. Absorbances of samples were measured spectrophotometrically at a wavelength of 570 nm, with background absorbance at 690 nm to determine cell viability. The treated cells were also measured for the viability with repect to time.

Results

Characteristics and stability of 16-nm sized MNP, MNP@SiO_2 particle with Dox, and liposome encapsulated MNP@*m*SiO_2 (MagLipo) particle

16-nm (diameter) iron oxide nanoparticles with a regular size distribution were simply synthesized by using a seed growing method (Fig. 1B) (*49,50*). Next, the mesoporous silica shell was successfully coated onto the surface of MNPs, which were treated with NH_4OH and TEOS. Resulting MNP@*m*SiO_2 particles clearly exhibited mesoporous morphology (Fig. 1C, high magnification image in Fig. 2A) and maintained the core MNP structure during the over-coating process. After mixing the MNP@*m*SiO_2 particle solution with phospholipid films, between 6 and 8 MNP@*m*SiO_2 particles were located inside the liposome, which make MagLipo particles, and were characterized by cryo-TEM analysis (Fig. 1D).

The MNP was characterized as having a typical ferrite spinel structure with powder X-ray diffraction and vibrating sample magnetometry revealed that it had a high M_s (95 emu/g[Fe]) with super-paramagnetism (Fig. 2B and C). The relaxivity measurements with TD-NMR (Minispec mq20, 0.47 T, Bruker) showed that the MNP particles had a relatively high r_2 (286 $mM^{-1}\cdot S^{-1}$). The r_2 value of mesoporous silica shell MNP (MNP@SiO_2) was comparable to the bare MNP (270 $mM^{-1}\cdot S^{-1}$), but much higher than the amorphous silica shell MNP (MNP@SiO_2, 70 $mM^{-1}\cdot S^{-1}$) (Fig. 2D and E).

The size distribution of the prepared nanoparticles (MNP, MNP@*m*SiO_2 and MagLipo) measured by DLS analysis showed relative monodispersity (Fig. 3A). The resistance of the mesoporous silica shell to acid corrosion was presented by dispersion of the MNP and MNP@*m*SiO_2 particles in a 1 N HCl solution (Fig. 3B). The bare MNPs quickly dissociated within 20 min (~50%), but the MNP@*m*SiO_2 particles showed remarkable stability and resistance. We thought that the resistance to the acidic etching was resulted from the ability of mesoporous silica trapping proton molecules into the shell by hydrogen bond formation. For biological applications, nanoparticles should be dispersed in buffer solution. However, the prepared MNP@*m*SiO_2 particles did not have high solubility in the PBS buffer solution. In contrast, the MagLipo particles were found to have long-term stability (Fig. 3C).

Loading efficiency of drug and therapeutic siRNA into MagLipo and controlled release of payload

The loading capacity of Dox was determined by HPLC analysis to be 98% (Fig. 4A). The *si*Plk1, prepared as complex with protamine (PA), was well loaded into the MagLipo and the loading efficiency of gene, analysed by UV-Vis spectroscopy (Fig. 4B), was approximately 80%. The MagLipo particles loaded with Dox, prepared with the NH_4HCO_3 gradient method, released 40% of Dox within 30 min in pH 4.7 solution (Figure 4C).

Antibody conjugated MagLipo and cytotoxicity study

The toxicological study of the MagLipo was conducted using fibroblast (293T, EGFR negative) and pancreatic cancer (BxPC3, EGFR positive) cell lines. Expression levels of EGFR in each cell lines were determined by western blotting. Both group of cells, separately treated with bare MagLipo and antibody conjugated MagLipo at different concentrations, showed high viability (> 85 %) after 24 h (Fig. 5A-C).

T_2-*w* MR phantom study

The EGFR-MagLipo-treated cells showed significant decrease in the T_2-*w* signal compared with the control (non-treated) and bare MagLipo (without antibody conjugation)-treated cells (Fig. 6A and B). The change in T_2 (ΔT_2 %), which is defined as the difference in T_2 between the cells treated with EGFR-MagLipo particles and the non-treated cells, is presented using a TD-NMR magnetic relaxometer (Fig. 6C) and the value found was approximately 10 cells if the threshold was chosen arbitrarily as 5% of ΔT_2, which is similar to the single cell level.

Delivery of therapeutic moieties

The EGFR positive BxPC3 cells were treated with the therapeutic EGFR-targeting

MagLipo particles for 3 hr and displayed progressive uptake of particles. With bio-TEM analysis of treated cells, the particles localized in the cytoplasm were identified (Fig. 7A, white arrows indicate particles). The location of the Dox in MagLipo was monitored with the confocal laser scanning microscope by its inherent red fluorescence property, and at initial stage, the red color from Dox was broadly distributed in the cytosol and diffused into the nucleus of the cell after continuous culture for 24 hr (Fig. 7B).

Cell viability assay

In the Plk1 expression level of various cells, which were analysed using the polymerase chain reaction (PCR) technique, cells treated with only *si*Plk1 showed a similar expression intensity as did the control (only cell). In contrast, the EGFR-MagLipo particles harboring both Dox and *si*Plk1 were shown to substantially down-regulate the Plk1, with an approximate 60% decrease compared with the control (Fig. 8A). More importantly, the MagLipo without an antibody showed minimal amount of inhibition on Plk1. In comparison of cell viability, as expected, the simultaneous incorporation of Dox and the *si*Plk1 into the MagLipo particle system was shown to have a remarkable induction effect on apoptotic cell death (~50%) after a 48-hr incubation (Fig. 8B) and reached ~70% of cell death after a 120-hr incubation. Compared with the single therapy with Dox-incorporated EGFR-MagLipo, simultaneous delivery with a drug and gene showed synergistic therapeutic effect.

Discussion

The theranostic applications of nanoparticles in the biomedical science have been in the spotlight for decades, and great anticipation of nanotheranostic platform readily applicable in the cancer treatment cannot be mentioned too often.

Metal nanoparticles of all are most promising candidate materials for the simultaneous diagnostic and therapeutic systems, not only because their innate properties are comparable as diagnostic and imaging purposes, also they could be sent to the cancer tissue or cells, armed with therapeutic drugs and equipped with targeting moiety. With these reasons, there exist several commercially available magnetic nanoparticles as contrast agents in magnetic resonance imaging, though magnetic sensing and magnetic hyperthermia will still need to be extensively validated before being introduced in the clinic, currently limited by the need of strong external magnetic field and by the concerns of sustained high temperature in the target organ along with a defined target volume, respectively (*51*).

Nanoparticles with iron oxide core, as an attractive platform in the biomedical field, have been widely and vigorously investigated for the various applications such as diagnostics, therapeutics, biosensing, drug delivery, and controlled release of drug (*52*). With their inherent superparamagnetism, iron oxide nanoparticles can be used as contrast agent for the diagnostic purpose in MRI imaging, supported by its high biocompatibility rarely causing oxidative stress (*53*). However, there are still increasing concerns about toxicity from reactive oxygen species (ROS) generated by nanoparticles and the toxicity from metallic core itself, especially of quantum dots (*11*,*54*), though standardized and systematized toxicity

studies area lacking (*10*,*55*). Therefore, surface passivation of iron oxide nanoparticle with silica is considered to play important role in reducing oxidative stress and alteration of iron homeostasis, and consequently, the overall toxicity (*56*). And more importantly, such a structures consists of iron oxide core and organic coating have shown to be efficient for the applications utilizing MRI.

Particularly, the mesoporous form of silica nanoparticles can be a good surface material of choice, because it could provide enough spaces for the loading of therapeutic drugs or genes, most importantly without compromising magnetic property of iron oxide core. Besides its several advantageous properties such as large surface area and pore volume to carry therapeutic moiety and favorable biocompatibility, the mesoporous silica is suggested to allow ready accessibility of water molecules to the magnetic core for the efficient water proton relaxation (*57*). In this study, the relaxivity of MNP@*m*SiO_2 was almost similar to that of bare MNPs, unlike with the low r_2 value of amorphous silica coated NPs, supporting the idea that the mesoporous silica can hold more water molecules than the amorphous silica can. Also, mesoporous silica nanoparticles are proposed as the basis of nanodevices for the controlled release of drugs and genes into living cells owing to its controllable morphology, porosity, and surface characteristics (*58*).

However, even with these several advantageous properties, generally, both amorphous and mesoporous silica coated core-shell particles do not have long-term stability (solubility) in buffer solutions. Therefore, the surface of *m*SiO_2 particles needs to be coated with hydrophilic materials. Among materials for the surface coating of nanoparticles, liposomal formulations have been most popular and efficient tool for the delivery of various therapeutic agents such as

chemotherapeutic drugs, oligonuclide, antigens, and proteins since it offers several favorable properties; biocompatibility, biodegradability, and low toxicity (*59,60*). Antibody targeted liposomes loaded with anticancer drugs demonstrated high potential for the clinical applications (*60*). Both passive and active drug delivery by liposomal nanoparticles can significantly reduce the toxic side effects of anticancer drugs and enhance therapeutic efficacy of the drug delivered (*61*). A meaningful progress is that the liposomes, with FDA approval, have been introduced and used as drug delivery system in clinic (Doxil, Abelcet, Ambisome) (*62,63*). Liposomal doxorubicin is indicated for ovarian cancer, breast cancer, multiple myeloma, and kaposi's sarcoma (*62*). Liposomal doxorubicin statistically trended to lower cardiac event rates than doxorubicin (*64*). The early and positive preclinical and clinical experiences with liposomal delivery of anthracyclines made liposome popular in nanomedicine for cancer therapy (*65*). Therefore, we combined a liposomal complex with biocompatible phospholipid chemicals as stabilizers. A novel structure of *m*SiO_2-coated MNP (MNP@*m*SiO_2) encapsulated liposomal particles (MagLipo) was prepared and showed good solubility in PBS buffer, suggesting this MagLipo particle system has excellent physico-chemical properties for biological applications. Despite their similar r_2 (270 $mM^{-1} \cdot S^{-1}$) values, the EGFR-MagLipo particles were shown to have a lower T_2 compared with MNP@*m*SiO_2 particles and it was assumed that the EGFR-MagLipo particles would have provided a much higher number of MNPs per one receptor of cell membrane than non-targeting particles, which would be akin to boosting cell uptake. Considering that the surface modifications need to be applied without compromising the magnetic property of iron oxide core, this unique feature of the MagLipo system in current study, even with amplified magnetism, can be regarded as very powerful and prominent

achievement from a diagnostic point of view. Based on the results from T_2-*w* signal phantom study, BxPC3 pancreatic cancer cells treated with the EGFR-MagLipo particles showed significantly lower signal intensity than control cells or cells treated with bare MagLipo did, meaning both selective targeting and successful T2 relaxation have been accomplished. In the application of in vitro magnetic sensing, namely cellular assay with EGFR-MagLipo system, the ΔT_2 change (%), defined as difference between cellular r_2 value of EGFR-MagLipo treated cells and of non-treated cells, showed that the only 10 EGFR-MagLipo-treated cells are required to be significantly differentiated from non-treated cells when 5% of ΔT_2 was set as threshold, suggesting that the MagLipo is an effective diagnostic material system for the in vitro sensing of pancreatic cancer cells.

Especially as a *si*RNA delivery system, liposomes can prevent degradation of payload, accumulate preferentially in tumor tissue, deliver high concentration of payload, and with active targeting moiety, it also can aid specific targeting of *si*RNAs to the tumor cells (34). The lipid nanoparticle formulation of a *si*RNA directed against Plk1, known as TKM-080301, successfully induced silencing of Plk1 expression in-vitro and in patient biopsy samples, and is being evaluated in a first-in-human, dose-escalation, phase I study in patients with advanced solid tumors (*41*). Among polo-like kinases (Plks), a family of serine-threonine kinases, Plk1 is the most widely understood key enzyme regulating essential steps of mitosis, overexpression of which in multiple human cancers and its association with poor prognosis have been well addressed (*34,36,37,66*). Since RNA interference with *si*RNA of Plk1 induced G2/M phase arrest and apoptosis in various cancer cell lines (*67*), strategies adopting depletion of Plk1 in cancer therapy were suggested as promising therapeutic approaches (*38-41*). The Plk1

inhibitor named as Volasertib is currently undergoing investigation in phase III clinical trial. Since cancer cells are often characterized as its notorious apoptosis resistance, treatment regimens combining both genetic silencing promoting apoptosis and chemotherapeutic drugs, if simultaneously and specifically delivered to the target tissues or cells, can be powerful and efficient strategies to maximize responsiveness of cancer to the therapy (*68*). As an example, the liposome-based polyplex combining TNF-α and doxorubicin was successfully targeted at the EGFR, which is overexpressed in tumor cells and showed synergistic therapeutic effect (*69*). In current study, to assign the cancer-specific theranostic properties to the MagLipo, the therapeutic drugs (Dox) and *si*RNAs (*si*Plk1) were incorporated into the particles, and the surface of MagLipo was modified with an antibody to the EGFR. The loading capacity for the chemotherapeutic agent (Dox) was significantly high as 98%, and delivery of Dox into the nucleus successfully proceeded. Encapsulation of *si*Plk1 in the MagLipo and silencing effect by this system were also well presented. These results highly suggest the capability of MagLipo as a drug delivery vehicle.

The acidic microenvironment of tumor, which is one of the reasons for the multidrug resistance, especially for weakly basic chemotherapeutic drug such as doxorubicin (*70*), has been most utilized intrinsic stimulus for the design of stimulus-sensitive nanopreparations (*71*). The local stimulus developed by the abnormal pH gradient from tumor's extracellular microenvironment (pH 6.5) to the intracellular organelles like endosome (pH 5.5) and lysosomes (below pH 5.5), plays an important role in the controlled release of the drugs after penetration into the cell (*71,72*). Controlled release of Dox and *si*Plk1 from the MagLipo system in acidic environment was nicely presented with minimal spillage of payload in

neutral pH. This may have been a result of the electrostatic interaction between the silicate (with a negative charge) and the Dox (with a positive charged). Pancreas cancer, the target disease in this study, is infamous for its aggressiveness, late presentation, and poor prognosis. Most pancreatic cancer patients are diagnosed in advanced stage and median survival of patients is less than 6 months (*73*). Even with multimodal therapies, pancreas cancer is one of the most common causes of cancer deaths (*74*). Outcomes of current study demonstrated that the synergistic apoptotic effect of nanoparticles carrying both Dox and *si*Plk1 on human pancreas cancer cells. Above mentioned processes and results of this study is well presented in the recently published article (*46*). Considering in vivo imaging studies conducted with iron oxide MNPs for a decade, some of them presented identifiable decrease in the signal intensity of targeted lesion on the MR images (*75,76*). However, heterogenous, even vague change of signal intensity (*77*) or small dot-like low intensity in relatively large lesion or indistinguishable small lesion itself (*78,79*) or pre- and post-contrast images that are not exactly same level of slices (*80*), have been said that the significant T2 relaxation had occurred. Dense nature of tumor stroma or disordered vasculature of tumor could have hindered the particles from getting into the tumor thoroughly. Most importantly, possible changes in the composition of nanoparticles after being administered to the human body have not been properly investigated yet. Uptake and distribution of nanoparticles in the body are complicated processes which cannot be fully evaluated in vitro system. Therefore, nanomedicine suffers from the tons of fancy results produced in the laboratory based analyses with basic shortage of reliable and reproducible in vivo data, which explains why most of nanoparticles rarely make its debut in clinical field. Even though iron oxide nanoparticles have been

considered as biocompatible based on the cellular viability tests, current information regarding its potential undesirable and unexpected adverse effects to the whole organism after exposure is scarce, and even existing results from in vitro studies are controversial. Thus, besides diagnostic and therapeutic performance, comprehensive toxicological information of nanoparticles is indispensable part of prerequisite for the biomedical application of MagLipo.

Consequently, this multifunctional nanovehicle, EGFR-targeted MagLipo particles showed considerable and synergistic therapeutic effect on pancreatic cancer cells and also displayed physicochemical properties good enough to be a contrast agent for MRI. We thus suggest that the co-delivery of Dox and *si*Plk1 using the MagLipo particle system is highly selective and efficient, which could provide a promising cancer therapy method to be translated from bench to bedside. Various nanoparticle systems have adopted iron oxide core, mesoporous silica, pH-responsive property, and simultaneous delivery of therapeutic genes and chemotherapeutic drugs, respectively or in the combination of two or more of them. Recent investigation presented a nanoparticle system combining mesoporous silica, pH-responsive drug delivery, and T_1-*w* magnetic resonance imaging (*81*). However, none of those formulations have all of the properties the MagLipo have. The ideal properties as a drug delivery system, which may be listed as longevity, targetability, stimuli-sensitivity, enhanced intracellular delivery, contrast property (*82*), and even the co-delivery system of therapeutic gene and chemotherapeutic agent, were all incorporated in current formulation, MagLipo, which make the particle unique and powerful as a nanovehicle in biomedical field. Despite its wide applications in nanomedicine, biodistribution of iron oxide nanoparticles was reported in few studies (*83-85*) and therefore, there are some concerns regarding its use in human

being (*18*). For the clinical application of MagLipo, comprehensive and deep understanding of its biocompatibility, toxicity, biodistribution, and in vivo targeting efficiency is mandatory.

CONCLUSIONS

In this study, we introduced the mesoporous silica shell onto the MNP to reduce oxidative stress from iron core while maintaining the magnetic property. Then, the MNP@*m*SiO_2 particles were combined with the liposomal complex system to improve solubility in the buffer solution. Finally, the EGFR antibody-anchored MagLipo particles were applied to BxPC3 pancreatic cancer cells for T_2-*w* MR imaging. These particles were detected in the single cancer cell level by magnetic sensing method and proved to be a sensitive diagnostic material. Furthermore, the therapeutic drug and gene could both be incorporated into the MagLipo particles and were released at low pH value that is the hallmark of cancer microenvironment. Co-delivery of Dox and *si*Plk1 using the EGFR-targeting MagLipo particle system showed highly selective and synergistic therapeutic effect for the treatment of pancreatic cancer cells. Combining attractive features of the theranostic nanoparticles all together, namely iron oxide core, mesoporous silica, pH-responsive property, and simultaneous delivery of therapeutic genes and chemotherapeutic drugs, a novel nanovehicle platform was proposed.

Based on these results, the MagLipo might be promising multifunctional nanovehicle for the specific cancer therapy and imaging at the same time. However, profound knowledge of potential toxicity and biodistribution of the nanoparticles at the organ and cellular levels after administration is indispensable for its application in clinic, as any techniques appeared flawless in vitro cannot guarantee stability, safety, and therapeutic efficacy in vivo system. There remains much to be done to predict what exactly will happen in human body after systemic application of nanoparticles. Currently, nanoparticles approved for clinical use are investigated in

large number of trials, and steady build-up of information regarding interaction and fate of nanoparticles extracted from those trials will provide basis for the validation of novel nanoparticle systems which are more advanced than currently approved ones. On condition that its path and fate in vivo system are clearly defined, it is expected that the MagLipo, as a smart and versatile nanoplatform that integrates imaging and therapeutic functions, will contribute to the advancement of highly specific and individualized treatment for cancer and simultaneous assessment of therapy response with image in the future.

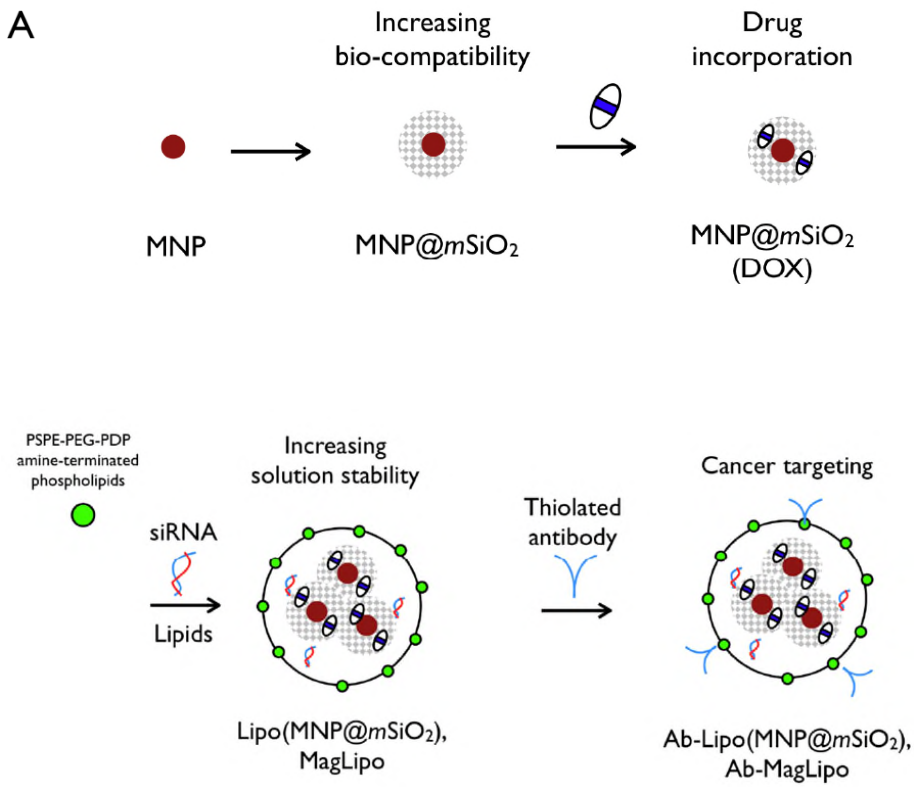
A
Increasing
bio-compatibility
Drug
incorporation
MNP
MNP@mSiO2
MNP@mSiO2
(DOX)
PSPE-PEG-PDP
amine-terminated
phospholipids
siRNA
Lipids
Increasing
solution stability
Lipo(MNP@mSiO2),
MagLipo
Thiolated
antibody
Cancer targeting
Ab-Lipo(MNP@mSiO2),
Ab-MagLipo

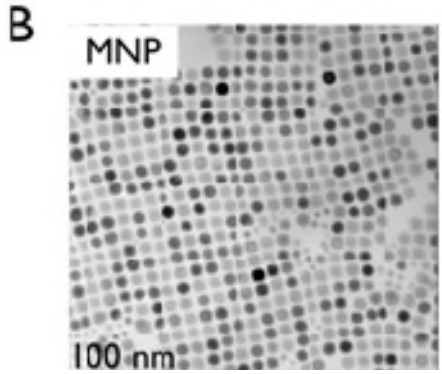
B
MNP
100 nm

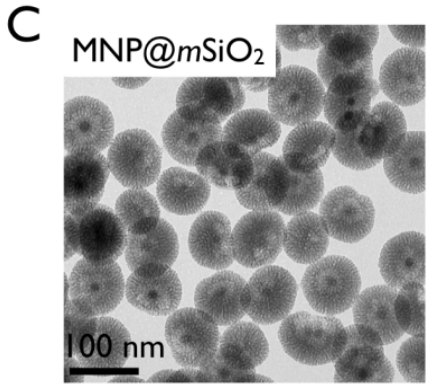
C
MNP@mSiO2
100 nm

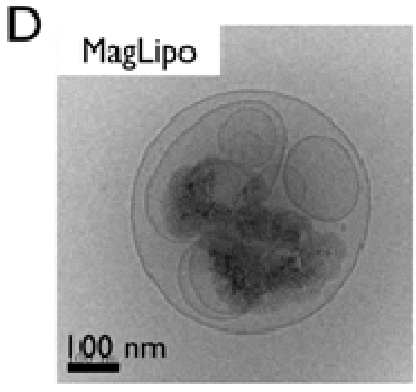
D
MagLipo
100 nm

Figure 1. Schematic illustration and TEM images of MagLipo

(A) Synthetic scheme of antibody-conjugated MagLipo particles.

(B) TEM images of the 16-nm iron oxide (Fe_3O_4) magnetic nanoparticles (MNPs) showed regular size distribution.

(C) TEM images of mesoporous silica shell coated iron oxide, MNP@*m*SiO_2 particles.

(D) High-magnification image of liposome encapsulated MNP@*m*SiO_2 particles, MagLipo.

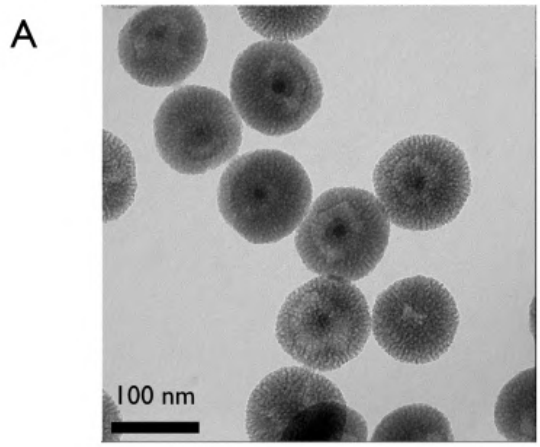
A
100 nm

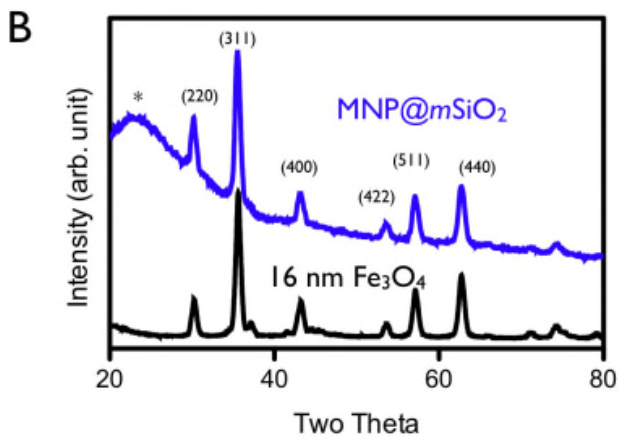
B
(311)
*
(220)
MNP@mSiO2
(400)
(511)
(422)
(440)
16 nm Fe3O4
Intensity (arb. unit)
20
40
60
80
Two Theta

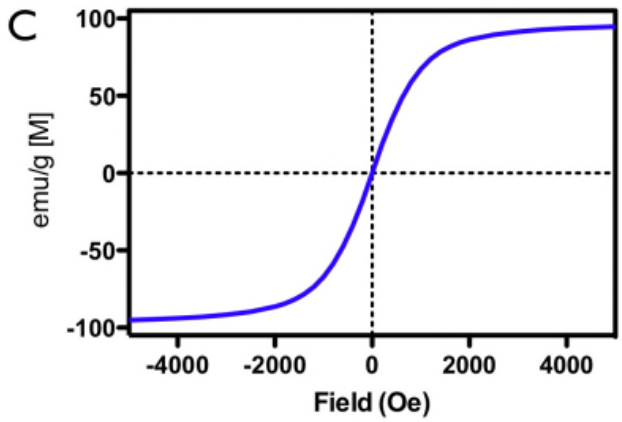
C
100
50
0
-50
-100
emu/g [M]
-4000
-2000
0
2000
4000
Field (Oe)

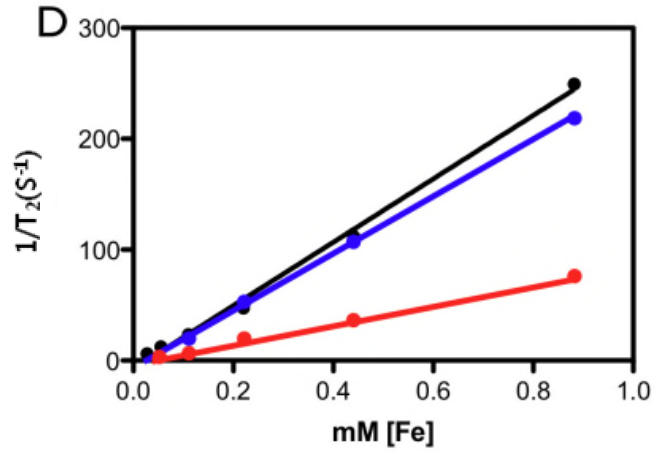

MNP (r_2 ~ 286 $mM^{-1} \cdot S^{-1}$)
MNP@mSiO$_2$ (r_2 ~ 270 $mM^{-1} \cdot S^{-1}$)
MNP@SiO$_2$ (r_2 ~ 70 $mM^{-1} \cdot S^{-1}$)

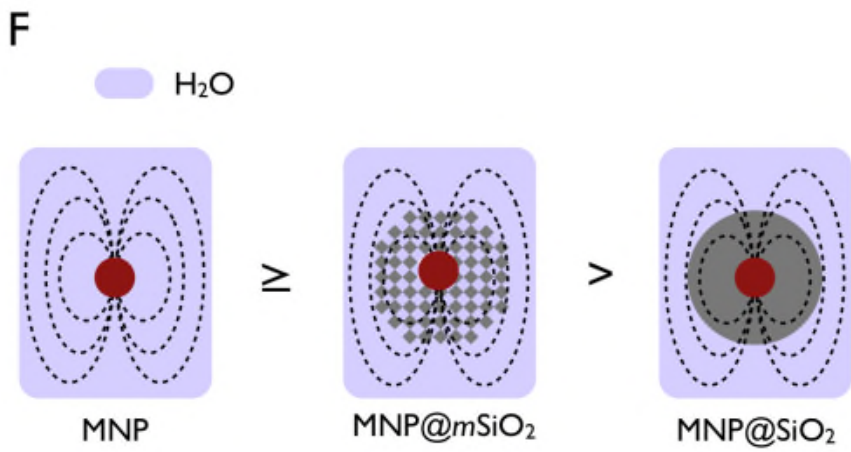

The number of water molecules under the magnetic field from MNP :
MNP ≥ MNP@mSiO$_2$ > MNP@SiO$_2$

Figure 2. Characteristics of various nanoparticles

(A) The morphology of MNP@*m*SiO_2 particles was clearly revealed porous shell from the high magnification image of TEM. (B) The structural information of 16-nm Fe_3O_4 nanoparticles (MNPs) and mesoporous silica shell coated MNPs characterized by powder X-ray diffraction (XRD) analysis. Typical inverse spinel structure was observed and MNP@*m*SiO_2 particle showed broad peak (marked with *) at the low angle resulting from the mesoporous silica shell. (C) The magnetic property of prepared MagLipo particles clearly showed super-paramagnetism and saturated magnetism with 95 emu/[Fe]g by Vibrating Sample Magnetometer (VSM). (D) The relaxivity of bare MNP, amorphous silica coated MNP (MNP@SiO_2), and mesoporous silica shell MNP (MNP@*m*SiO_2) were measured as 286, 70, and 270 $mM^{-1}{\cdot}S^{-1}$ respectively by using of TD-NMR (D, Minispec mq20, 0.47 T, Bruker). From the results, the amorphous silica shell (red line) caused decrease in magnetic relaxation, which might be due to the reduced number of water molecules around the MNPs. However, the mesoporous silica shell coated MNPs (blue line) showed relatively higher relaxivity then the amorphous silica shell coated particles and similar relaxivity (r_2) value with that of bare MNPs (black line). (E) Illustration of water molecules in the magnetic field in the vicinity of MNP core. The mesoporous silica shell is assumed to possess water molecules nearby the MNP magnetic field.

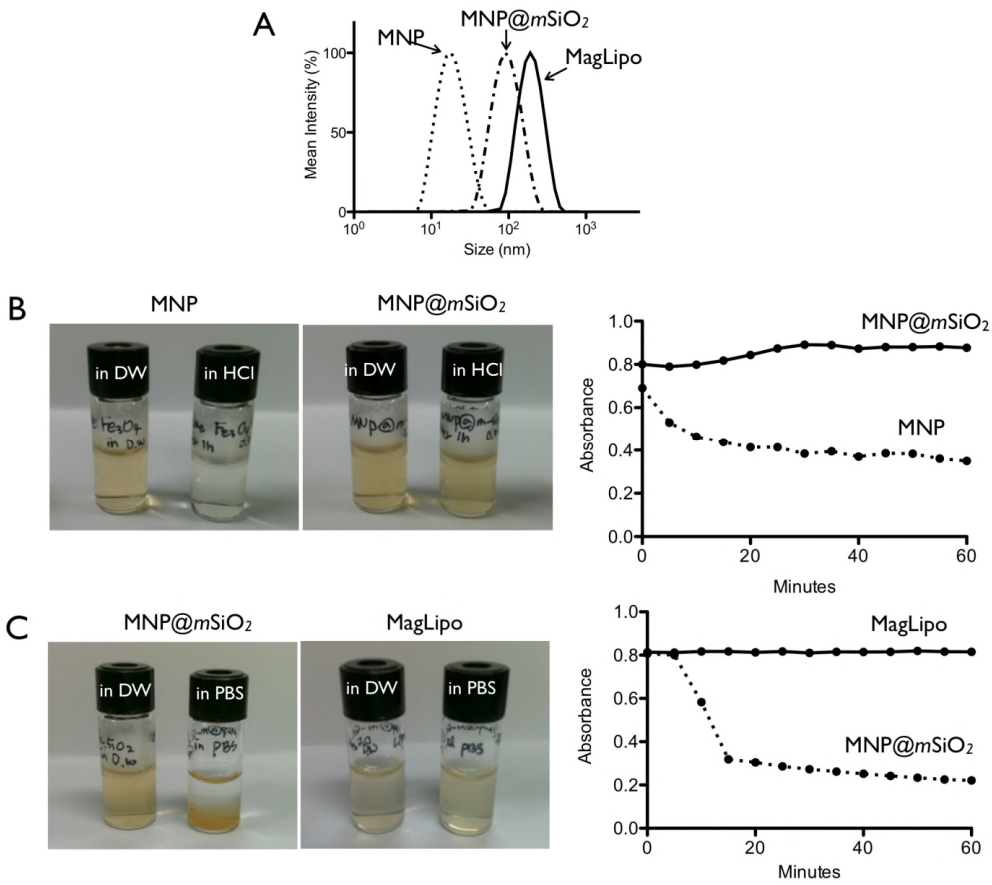
A
MNP
MNP@mSiO2
MagLipo
Mean Intensity (%)
100
50
0
10^0
10^1
10^2
10^3
Size (nm)
B
MNP
MNP@mSiO2
in DW
in HCl
in DW
in HCl
MNP@mSiO2
MNP
Absorbance
1.0
0.8
0.6
0.4
0.2
0.0
0
20
40
60
Minutes
C
MNP@mSiO2
MagLipo
in DW
in PBS
in DW
in PBS
MagLipo
MNP@mSiO2
Absorbance
1.0
0.8
0.6
0.4
0.2
0.0
0
20
40
60
Minutes

Figure 3. Solution stability of nanoparticles in various conditions

(A) Size distributions of the prepared nanoparticles (MNP, MNP@*m*SiO_2 and MagLipo) were measured by dynamic light scattering (DLS) analysis and showed relative monodispersity. (B) The water soluble bare MNPs were dissociated in the 1 N HCl solutions within 20 min, but the mesoporous silica shell effectively protected the MNP core in the same condition. (C) Nanoparticles should be dispersed in buffer solution for biological application. The prepared MNP@*m*SiO_2 particles showed poor solubility in PBS buffer solution and precipitated within 15 min. But the MagLipo particles exhibited high stability and solubility in PBS solution. The absorbance was determined at 450 nm by UV-Vis spectroscopy.

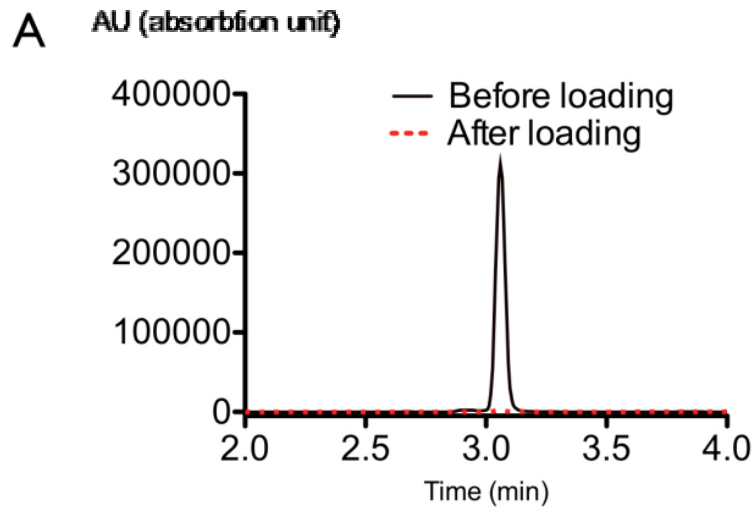
A
AU (absorbfion unif)
400000
300000
200000
100000
0
Before loading
After loading
2.0
2.5
3.0
3.5
4.0
Time (min)

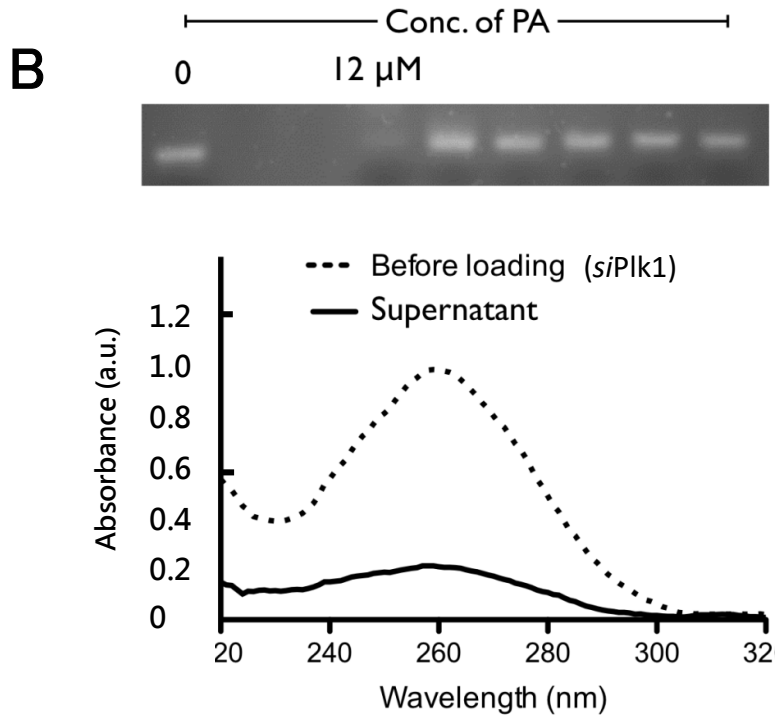
B
Conc. of PA
0
12 μM
Before loading (siPlk1)
Supernatant
Absorbance (a.u.)
1.2
1.0
0.8
0.6
0.4
0.2
0
20
240
260
280
300
320
Wavelength (nm)

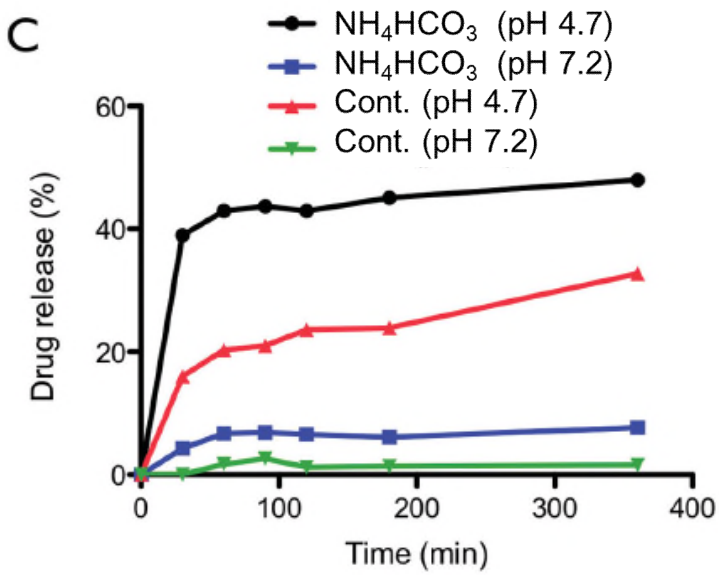
C
NH4HCO3 (pH 4.7)
NH4HCO3 (pH 7.2)
Cont. (pH 4.7)
Cont. (pH 7.2)
Drug release (%)
60
40
20
0
0
100
200
300
400
Time (min)

Figure 4. Characterization of drug or siRNA incorporation and controlled release

(A) The therapeutic drug (doxorubicin, Dox) was incorporated easily into the mesoporous silica coated MNP and the loading capacity was determined to be 98% by HPLC analysis. The supernatant solution after loading was analyzed for the amount of Dox concentration. (B) The *si*Plk1 with negative charge was first complexed with positively charged protamine protein (PA) based on electrostatic interaction and then incorporated into the MagLipo using the NH_4HCO_3 gradient method. The ratio of *si*Plk1 and PA was optimized to 1.5 siRNAs per PA using an electrophoretic protocol. The loading capacity measured with UV-Vis spectroscopy was 80%. (C) For pH-sensitive controlled release of incorporated therapeutic materials, the MagLipo particles were exposed to acidic conditions (pH 4.7) and found to quickly release Dox in NH_4HCO_3 gradient samples (control indicates samples without NH_4HCO_3 gradient) showing 40% release of Dox within 30 min, which is satisfactory for therapeutics.

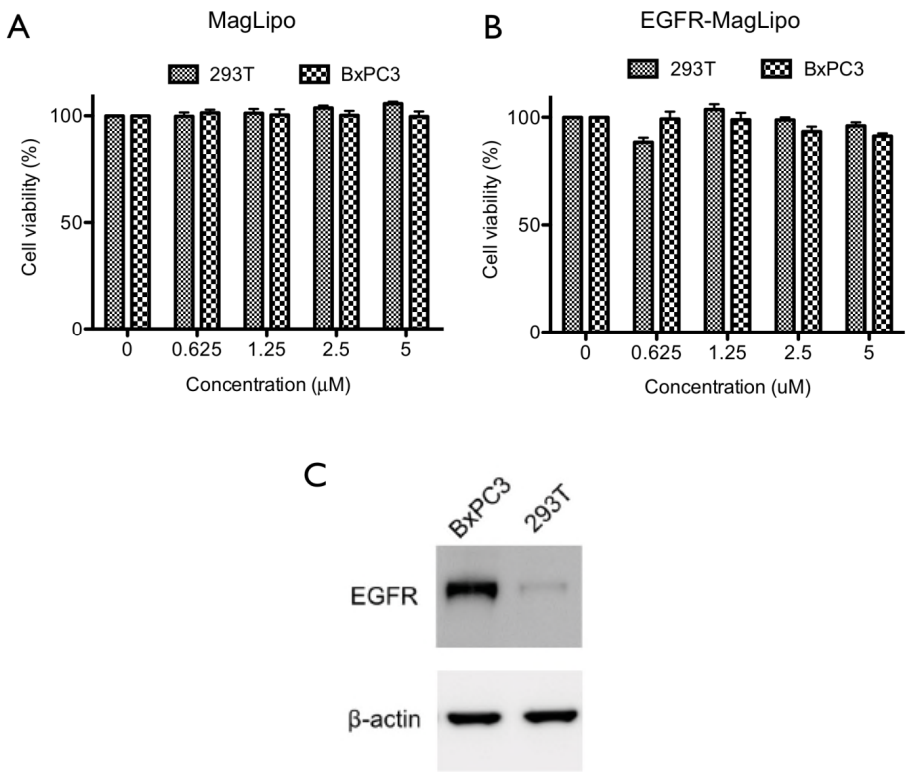
A
MagLipo
293T
BxPC3
Cell viability (%)
100
50
0
0
0.625
1.25
2.5
5
Concentration (μM)
B
EGFR-MagLipo
293T
BxPC3
Cell viability (%)
100
50
0
0
0.625
1.25
2.5
5
Concentration (uM)
C
BxPC3
293T
EGFR
β-actin

Figure 5. Assessment of cell cytotoxicity and expression level of EGFR receptor

(A and B) MagLipo (A) and EGFR antibody-conjugated MagLipo (EGFR-MagLipo) (B) showed high cell viability (< 90%) in the 293T and BxPC3 cell lines after treatment with various concentrations of particle solution for 3 hr. 293T is an embryonic kidney cell line (ATCC) and EGFR negative. BxPC3 is EGFR positive pancreatic cancer cell line. (C) The expression level of EGFR marker receptor protein was characterized by western blotting. The pancreatic cancer (BxPC3) was shown to be a positive cell line with EGFR. And 293T were determined as EGFR-negative cell line.

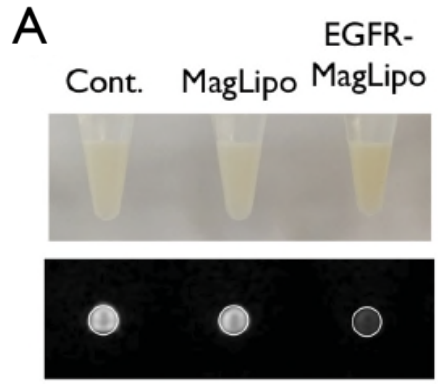
A
Cont.
MagLipo
EGFR-
MagLipo

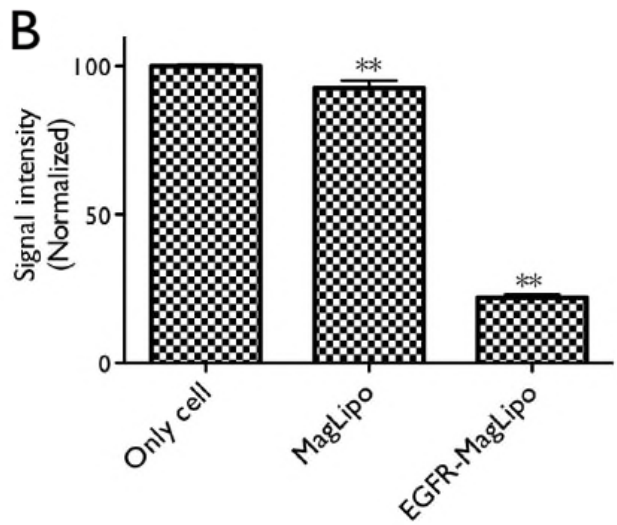
B
Signal intensity
(Normalized)
100
50
0
**
**
Only cell
MagLipo
EGFR-MagLipo

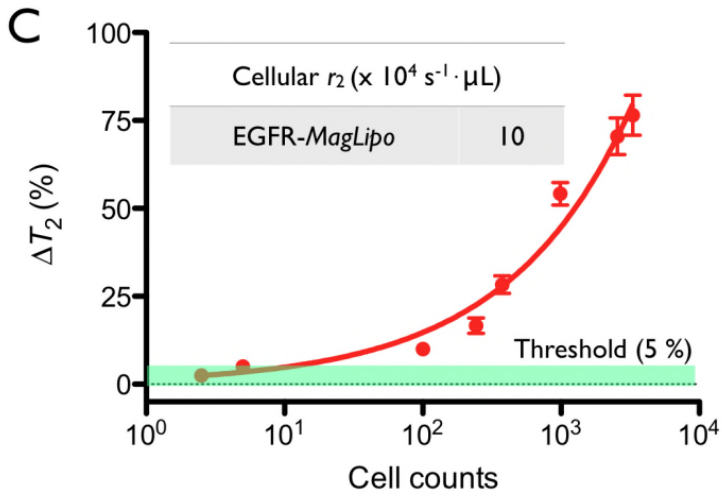
C
100
75
50
25
0
ΔT2 (%)
Cellular r2 (x 10^4 s^-1 · μL)
EGFR-MagLipo
10
Threshold (5 %)
10^0
10^1
10^2
10^3
10^4
Cell counts

Figure 6. Magnetic property of MagLipo

(A) After being treated with the particles, the EGFR-positive BxPC3 cells were imaged by T_2- *w* MR as a phantom study. (B) Non antibody-conjugated MagLipo showed similar intensity as the control (nontreated) cells, but the EGFR-MagLipo-treated cells exhibited significantly enhanced black contrast imaging with ≈80% decreasing T2 values (data are presented as the mean ± SE from triplicate measurements,** $p < 0.01$). (C) Quantitative magnetic cellular relaxivity for the sensitivity measurements after treatment with EGFR-MagLipo particles. The ΔT_2 % change was the difference in T2 between the EGFR-MagLipo particle-treated cells and the non-treated cells.

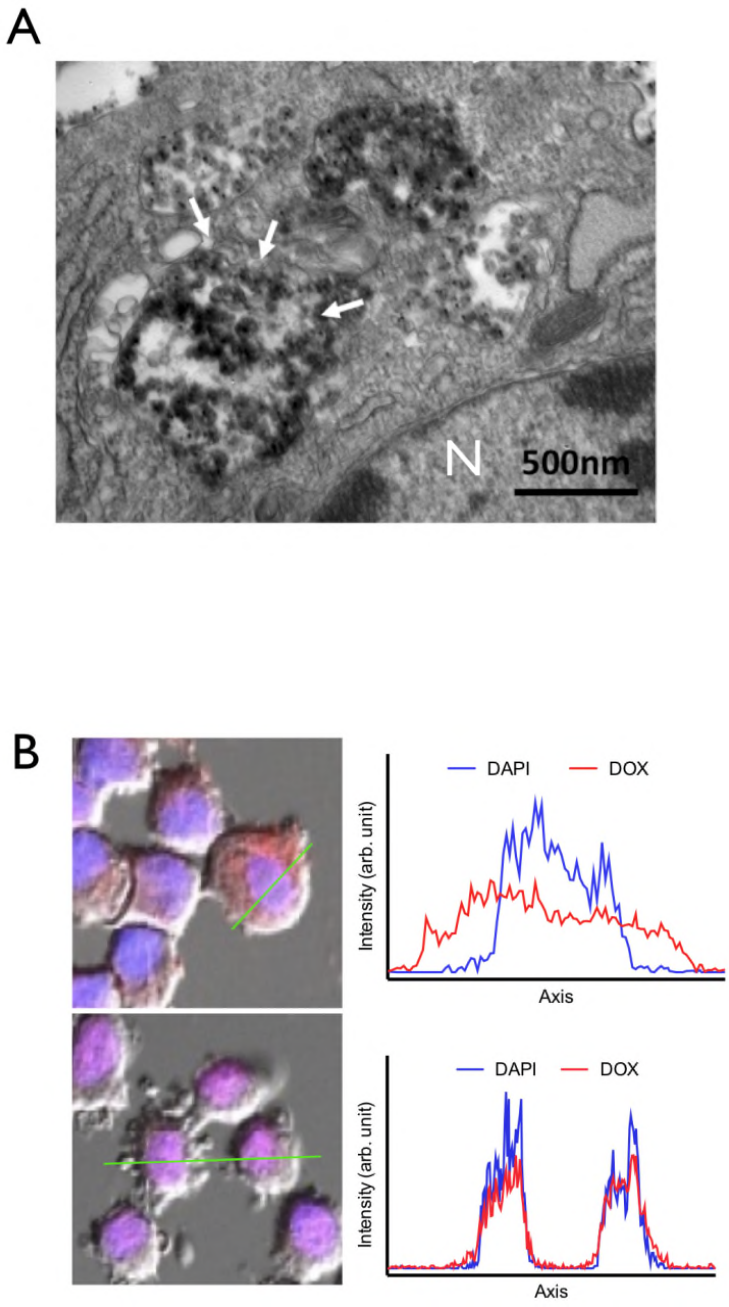
A
N
500nm
B
DAPI
DOX
Intensity (arb. unit)
Axis
DAPI
DOX
Intensity (arb. unit)
Axis

Figure 7. Uptake of MagLipo particles in the cell

(A) Bio-TEM images showed penetrated particles in the cytosol of BxPC3 cell (white arrows;

N indicates nucleus). B) The location of Dox after treatment was monitored during delivery by confocal laser scanning microscopy. Images and line profiles are shown directly after administration (top) and 24 hr after administration (bottom). Red indicates the Dox, and the nucleus was stained with DAPI agent to blue color. Plot of intensity profiles along the green lines in the microscopic images are given on the right for red and blue color intensity. After 24 hr, the red and blue were perfectly matched, showing the ability of delivered Dox to penetrate the nucleus.

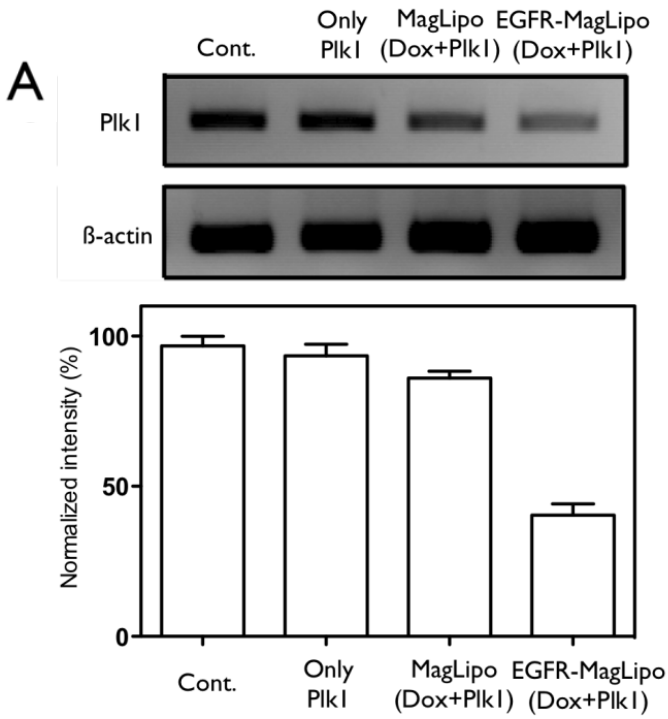
A
Cont.
Only Plk1
MagLipo (Dox+Plk1)
EGFR-MagLipo (Dox+Plk1)
Plk1
ß-actin
Normalized intensity (%)
100
50
0
Cont.
Only Plk1
MagLipo (Dox+Plk1)
EGFR-MagLipo (Dox+Plk1)

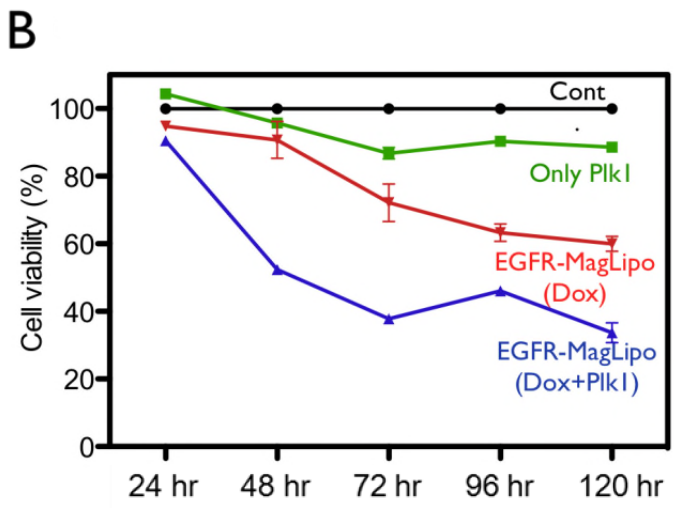
B
Cell viability (%)
100
80
60
40
20
0
24 hr
48 hr
72 hr
96 hr
120 hr
Cont
Only Plk1
EGFR-MagLipo (Dox)
EGFR-MagLipo (Dox+Plk1)

Figure 8. Therapeutic applications of MagLipo particles in vitro

(A) The efficiency of *si*Plk1 delivery was characterized by PCR analysis of treated cells and Plk1 was effectively downregulated in the EGFR-MagLipo-treated cells with a 60% decrease (data are the mean ± SE from triplicate measurements, ** $p < 0.01$).

(B) The treated cells were measured for the viability to evaluate the therapeutic effects with respect to time.

References

1. Yoon YI, Ju KY, Cho HS, et al. Enhancement of cancer specific delivery using ultrasound active bio-originated particles. *Chem Commun (Camb).* 2015;51:9455-9458.

2. Cole JT, Holland NB. Multifunctional nanoparticles for use in theranostic applications. *Drug Deliv Transl Res.* 2015;5:295-309.

3. Oliveira ON, Jr., Iost RM, Siqueira JR, Jr., Crespilho FN, Caseli L. Nanomaterials for diagnosis: challenges and applications in smart devices based on molecular recognition. *ACS Appl Mater Interfaces.* 2014;6:14745-14766.

4. Shi D, Sadat ME, Dunn AW, Mast DB. Photo-fluorescent and magnetic properties of iron oxide nanoparticles for biomedical applications. *Nanoscale.* 2015;7:8209-8232.

5. Lammers T, Aime S, Hennink WE, Storm G, Kiessling F. Theranostic nanomedicine. *Acc Chem Res.* 2011;44:1029-1038.

6. Siddiqi KS, Ur Rahman A, Tajuddin, Husen A. Biogenic Fabrication of Iron/Iron Oxide Nanoparticles and Their Application. *Nanoscale Res Lett.* 2016;11:498.

7. Min H, Jo SM, Kim HS. Efficient capture and simple quantification of circulating tumor cells using quantum dots and magnetic beads. *Small.* 2015;11:2536-2542.

8. Xing X, Zhang B, Wang X, Liu F, Shi D, Cheng Y. An "imaging-biopsy" strategy for colorectal tumor reconfirmation by multipurpose paramagnetic quantum dots. *Biomaterials.* 2015;48:16-25.

9. Ding D, Goh CC, Feng G, et al. Ultrabright organic dots with aggregation-induced

emission characteristics for real-time two-photon intravital vasculature imaging. *Adv Mater.* 2013;25:6083-6088.

10. Tsoi KM, Dai Q, Alman BA, Chan WC. Are quantum dots toxic? Exploring the discrepancy between cell culture and animal studies. *Acc Chem Res.* 2013;46:662-671.

11. Nguyen KC, Willmore WG, Tayabali AF. Cadmium telluride quantum dots cause oxidative stress leading to extrinsic and intrinsic apoptosis in hepatocellular carcinoma HepG2 cells. *Toxicology.* 2013;306:114-123.

12. Law WC, Yong KT, Roy I, et al. Aqueous-phase synthesis of highly luminescent CdTe/ZnTe core/shell quantum dots optimized for targeted bioimaging. *Small.* 2009;5:1302-1310.

13. Liu X, Wang Q, Li C, et al. Cu(2)-xSe@mSiO(2)-PEG core-shell nanoparticles: a low-toxic and efficient difunctional nanoplatform for chemo-photothermal therapy under near infrared light radiation with a safe power density. *Nanoscale.* 2014;6:4361-4370.

14. Yoon TJ, Yu KN, Kim E, et al. Specific targeting, cell sorting, and bioimaging with smart magnetic silica core-shell nanomaterials. *Small.* 2006;2:209-215.

15. Hilger I, Kaiser WA. Iron oxide-based nanostructures for MRI and magnetic hyperthermia. *Nanomedicine (Lond).* 2012;7:1443-1459.

16. Paik SY, Kim JS, Shin SJ, Ko S. Characterization, Quantification, and Determination of the Toxicity of Iron Oxide Nanoparticles to the Bone Marrow Cells. *Int J Mol Sci.* 2015;16:22243-22257.

17. Jeng HA, Swanson J. Toxicity of metal oxide nanoparticles in mammalian cells. *J*

Environ Sci Health A Tox Hazard Subst Environ Eng. 2006;41:2699-2711.

18. Ali A, Zafar H, Zia M, et al. Synthesis, characterization, applications, and challenges of iron oxide nanoparticles. *Nanotechnol Sci Appl.* 2016;9:49-67.

19. Liong M, Im H, Majmudar MD, et al. Magnetic ligation method for quantitative detection of microRNAs. *Adv Healthc Mater.* 2014;3:1015-1019.

20. Chen Y, Xianyu Y, Wang Y, et al. One-step detection of pathogens and viruses: combining magnetic relaxation switching and magnetic separation. *ACS Nano.* 2015;9:3184-3191.

21. York JN, Albanese C, Rodriguez O, Le YC, Ackun-Farmmer M, Van Keuren E. The effects of particle shape and size on T2 relaxation in magnetic resonance imaging. *J Biomed Nanotechnol.* 2014;10:3392-3396.

22. Yoon TJ, Lee H, Shao H, Weissleder R. Highly magnetic core-shell nanoparticles with a unique magnetization mechanism. *Angew Chem Int Ed Engl.* 2011;50:4663-4666.

23. Yoon TJ, Lee H, Shao H, Hilderbrand SA, Weissleder R. Multicore assemblies potentiate magnetic properties of biomagnetic nanoparticles. *Adv Mater.* 2011;23:4793-4797.

24. Cha J, Kwon YS, Yoon TJ, Lee JK. Relaxivity control of magnetic nanoclusters for efficient magnetic relaxation switching assay. *Chem Commun (Camb).* 2013;49:457-459.

25. Smolensky ED, Park HY, Zhou Y, et al. Scaling Laws at the Nano Size: The Effect of Particle Size and Shape on the Magnetism and Relaxivity of Iron Oxide Nanoparticle Contrast Agents. *J Mater Chem B Mater Biol Med.* 2013;1:2818-2828.

26. Wu W, He Q, Jiang C. Magnetic iron oxide nanoparticles: synthesis and surface functionalization strategies. *Nanoscale Res Lett.* 2008;3:397-415.

27. Mao X, Xu J, Cui H. Functional nanoparticles for magnetic resonance imaging. *Wiley Interdiscip Rev Nanomed Nanobiotechnol.* 2016;8:814-841.

28. Hurley KR, Lin YS, Zhang J, Egger SM, Haynes CL. Effects of mesoporous silica coating and post-synthetic treatment on the transverse relaxivity of iron oxide nanoparticles. *Chem Mater.* 2013;25:1968-1978.

29. Minotti G, Menna P, Salvatorelli E, Cairo G, Gianni L. Anthracyclines: molecular advances and pharmacologic developments in antitumor activity and cardiotoxicity. *Pharmacol Rev.* 2004;56:185-229.

30. Peng X, Chen B, Lim CC, Sawyer DB. The cardiotoxicology of anthracycline chemotherapeutics: translating molecular mechanism into preventative medicine. *Mol Interv.* 2005;5:163-171.

31. Barenholz Y. Doxil(R)--the first FDA-approved nano-drug: lessons learned. *J Control Release.* 2012;160:117-134.

32. Dai X, Yue Z, Eccleston ME, Swartling J, Slater NK, Kaminski CF. Fluorescence intensity and lifetime imaging of free and micellar-encapsulated doxorubicin in living cells. *Nanomedicine.* 2008;4:49-56.

33. Yu C, Zhang X, Sun G, et al. RNA interference-mediated silencing of the polo-like kinase 1 gene enhances chemosensitivity to gemcitabine in pancreatic adenocarcinoma cells. *J Cell Mol Med.* 2008;12:2334-2349.

34. Wolf G, Elez R, Doermer A, et al. Prognostic significance of polo-like kinase (PLK) expression in non-small cell lung cancer. *Oncogene.* 1997;14:543-549.

35. Knecht R, Elez R, Oechler M, Solbach C, von Ilberg C, Strebhardt K. Prognostic significance of polo-like kinase (PLK) expression in squamous cell carcinomas of the head and neck. *Cancer Res.* 1999;59:2794-2797.

36. Takahashi T, Sano B, Nagata T, et al. Polo-like kinase 1 (PLK1) is overexpressed in primary colorectal cancers. *Cancer Sci.* 2003;94:148-152.

37. Wang ZX, Xue D, Liu ZL, et al. Overexpression of polo-like kinase 1 and its clinical significance in human non-small cell lung cancer. *Int J Biochem Cell Biol.* 2012;44:200-210.

38. Yim H, Erikson RL. Polo-like kinase 1 depletion induces DNA damage in early S prior to caspase activation. *Mol Cell Biol.* 2009;29:2609-2621.

39. Xu WJ, Zhang S, Yang Y, et al. Efficient inhibition of human colorectal carcinoma growth by RNA interference targeting polo-like kinase 1 in vitro and in vivo. *Cancer Biother Radiopharm.* 2011;26:427-436.

40. Yoon HE, Kim SA, Choi HS, Ahn MY, Yoon JH, Ahn SG. Inhibition of Plk1 and Pin1 by 5'-nitro-indirubinoxime suppresses human lung cancer cells. *Cancer Lett.* 2012;316:97-104.

41. Liu X. Targeting Polo-Like Kinases: A promising therapeutic approach for cancer treatment. *Transl Oncol.* 2015;8:185-195.

42. Fang J, Nakamura H, Maeda H. The EPR effect: Unique features of tumor blood vessels for drug delivery, factors involved, and limitations and augmentation of the effect. *Adv Drug Deliv Rev.* 2011;63:136-151.

43. Zhang C, Yan Y, Zou Q, Chen J, Li C. Superparamagnetic iron oxide nanoparticles for MR imaging of pancreatic cancer: Potential for early diagnosis through targeted

strategies. *Asia Pac J Clin Oncol.* 2016;12:13-21.

44. Bakhtiary Z, Saei AA, Hajipour MJ, Raoufi M, Vermesh O, Mahmoudi M. Targeted superparamagnetic iron oxide nanoparticles for early detection of cancer: Possibilities and challenges. *Nanomedicine.* 2016;12:287-307.

45. Xiong HQ, Abbruzzese JL. Epidermal growth factor receptor-targeted therapy for pancreatic cancer. *Semin Oncol.* 2002;29:31-37.

46. Kwon YS, Jang SJ, Yoon YI, et al. Magnetic liposomal particles for magnetic imaging, sensing, and the pH-sensitive delivery of therapeutics. *Particle and Particle systems characterization.* 2016;33:242-247.

47. Liu J, Ma H, Wei T, Liang XJ. CO_2 gas induced drug release from pH-sensitive liposome to circumvent doxorubicin resistant cells. *Chem Commun (Camb).* 2012;48:4869-4871.

48. Chung MF, Chen KJ, Liang HF, et al. A liposomal system capable of generating CO_2 bubbles to induce transient cavitation, lysosomal rupturing, and cell necrosis. *Angew Chem Int Ed Engl.* 2012;51:10089-10093.

49. Sun S, Zeng H, Robinson DB, et al. Monodisperse MFe_2O_4 (M = Fe, Co, Mn) nanoparticles. *J Am Chem Soc.* 2004;126:273-279.

50. Lee H, Yoon TJ, Figueiredo JL, Swirski FK, Weissleder R. Rapid detection and profiling of cancer cells in fine-needle aspirates. *Proc Natl Acad Sci U S A.* 2009;106:12459-12464.

51. Singh A, Sahoo SK. Magnetic nanoparticles: a novel platform for cancer theranostics. *Drug Discov Today.* 2014;19:474-481.

52. Tran PH, Tran TT, Vo TV, Lee BJ. Promising iron oxide-based magnetic

nanoparticles in biomedical engineering. *Arch Pharm Res.* 2012;35:2045-2061.

53. Hohnholt MC, Geppert M, Dringen R. Treatment with iron oxide nanoparticles induces ferritin synthesis but not oxidative stress in oligodendroglial cells. *Acta Biomater.* 2011;7:3946-3954.

54. Han SG, Newsome B, Hennig B. Titanium dioxide nanoparticles increase inflammatory responses in vascular endothelial cells. *Toxicology.* 2013;306:1-8.

55. Valdiglesias V, Fernandez-Bertolez N, Kilic G, et al. Are iron oxide nanoparticles safe? Current knowledge and future perspectives. *J Trace Elem Med Biol.* 2016;38:53-63.

56. Malvindi MA, De Matteis V, Galeone A, et al. Toxicity assessment of silica coated iron oxide nanoparticles and biocompatibility improvement by surface engineering. *PLoS One.* 2014;9:e85835.

57. Kim JS, Rieter WJ, Taylor KM, An H, Lin W, Lin W. Self-assembled hybrid nanoparticles for cancer-specific multimodal imaging. *J Am Chem Soc.* 2007;129:8962-8963.

58. Trewyn BG, Slowing, II, Giri S, Chen HT, Lin VS. Synthesis and functionalization of a mesoporous silica nanoparticle based on the sol-gel process and applications in controlled release. *Acc Chem Res.* 2007;40:846-853.

59. Ozpolat B, Sood AK, Lopez-Berestein G. Liposomal siRNA nanocarriers for cancer therapy. *Adv Drug Deliv Rev.* 2014;66:110-116.

60. Sawant RR, Torchilin VP. Challenges in development of targeted liposomal therapeutics. *AAPS J.* 2012;14:303-315.

61. Zhao G, Rodriguez BL. Molecular targeting of liposomal nanoparticles to tumor

microenvironment. *Int J Nanomedicine.* 2013;8:61-71.

62. Duggan ST, Keating GM. Pegylated liposomal doxorubicin: a review of its use in metastatic breast cancer, ovarian cancer, multiple myeloma and AIDS-related Kaposi's sarcoma. *Drugs.* 2011;71:2531-2558.

63. Petros RA, DeSimone JM. Strategies in the design of nanoparticles for therapeutic applications. *Nat Rev Drug Discov.* 2010;9:615-627.

64. Yamaguchi N, Fujii T, Aoi S, Kozuch PS, Hortobagyi GN, Blum RH. Comparison of cardiac events associated with liposomal doxorubicin, epirubicin and doxorubicin in breast cancer: a Bayesian network meta-analysis. *Eur J Cancer.* 2015;51:2314-2320.

65. Gabizon AA, Patil Y, La-Beck NM. New insights and evolving role of pegylated liposomal doxorubicin in cancer therapy. *Drug Resist Updat.* 2016;29:90-106.

66. Han DP, Zhu QL, Cui JT, et al. Polo-like kinase 1 is overexpressed in colorectal cancer and participates in the migration and invasion of colorectal cancer cells. *Med Sci Monit.* 2012;18:BR237-246.

67. Spankuch-Schmitt B, Bereiter-Hahn J, Kaufmann M, Strebhardt K. Effect of RNA silencing of polo-like kinase-1 (PLK1) on apoptosis and spindle formation in human cancer cells. *J Natl Cancer Inst.* 2002;94:1863-1877.

68. Li J, Wang Y, Zhu Y, Oupicky D. Recent advances in delivery of drug-nucleic acid combinations for cancer treatment. *J Control Release.* 2013;172:589-600.

69. Su B, Cengizeroglu A, Farkasova K, et al. Systemic TNFalpha gene therapy synergizes with liposomal doxorubicine in the treatment of metastatic cancer. *Mol Ther.* 2013;21:300-308.

70. Wojtkowiak JW, Verduzco D, Schramm KJ, Gillies RJ. Drug resistance and cellular adaptation to tumor acidic pH microenvironment. *Mol Pharm.* 2011;8:2032-2038.

71. Zhu L, Torchilin VP. Stimulus-responsive nanopreparations for tumor targeting. *Integr Biol (Camb).* 2013;5:96-107.

72. Crayton SH, Tsourkas A. pH-titratable superparamagnetic iron oxide for improved nanoparticle accumulation in acidic tumor microenvironments. *ACS Nano.* 2011;5:9592-9601.

73. Jemal A, Siegel R, Xu J, Ward E. Cancer statistics, 2010. *CA Cancer J Clin.* 2010;60:277-300.

74. Kimple RJ, Russo S, Monjazeb A, Blackstock AW. The role of chemoradiation for patients with resectable or potentially resectable pancreatic cancer. *Expert Rev Anticancer Ther.* 2012;12:469-480.

75. Huh YM, Jun YW, Song HT, et al. In vivo magnetic resonance detection of cancer by using multifunctional magnetic nanocrystals. *J Am Chem Soc.* 2005;127:12387-12391.

76. Yu MK, Jeong YY, Park J, et al. Drug-loaded superparamagnetic iron oxide nanoparticles for combined cancer imaging and therapy in vivo. *Angew Chem Int Ed Engl.* 2008;47:5362-5365.

77. Yang L, Mao H, Wang YA, et al. Single chain epidermal growth factor receptor antibody conjugated nanoparticles for in vivo tumor targeting and imaging. *Small.* 2009;5:235-243.

78. Medarova Z, Pham W, Kim Y, Dai G, Moore A. In vivo imaging of tumor

response to therapy using a dual-modality imaging strategy. *Int J Cancer.* 2006;118:2796-2802.

79. Xie J, Chen K, Lee HY, et al. Ultrasmall c(RGDyK)-coated Fe_3O_4 nanoparticles and their specific targeting to integrin alpha(v)beta3-rich tumor cells. *J Am Chem Soc.* 2008;130:7542-7543.

80. Torres Martin de Rosales R, Tavare R, Paul RL, et al. Synthesis of ^{64}Cu(II)-bis(dithiocarbamatebisphosphonate) and its conjugation with superparamagnetic iron oxide nanoparticles: in vivo evaluation as dual-modality PET-MRI agent. *Angew Chem Int Ed Engl.* 2011;50:5509-5513.

81. Chen Y, Ai K, Liu J, Sun G, Yin Q, Lu L. Multifunctional envelope-type mesoporous silica nanoparticles for pH-responsive drug delivery and magnetic resonance imaging. *Biomaterials.* 2015;60:111-120.

82. Torchilin V. Multifunctional and stimuli-sensitive pharmaceutical nanocarriers. *Eur J Pharm Biopharm.* 2009;71:431-444.

83. Jain TK, Reddy MK, Morales MA, Leslie-Pelecky DL, Labhasetwar V. Biodistribution, clearance, and biocompatibility of iron oxide magnetic nanoparticles in rats. *Mol Pharm.* 2008;5:316-327.

84. Edge D, Shortt CM, Gobbo OL, et al. Pharmacokinetics and bio-distribution of novel super paramagnetic iron oxide nanoparticles (SPIONs) in the anaesthetized pig. *Clin Exp Pharmacol Physiol.* 2016;43:319-326.

85. Ruiz A, Hernandez Y, Cabal C, et al. Biodistribution and pharmacokinetics of uniform magnetite nanoparticles chemically modified with polyethylene glycol. *Nanoscale.* 2013;5:11400-11408.

Abstract

Liposomal delivery of mesoporous silica-coated iron oxide magnetic nanoparticles for theranostic application

Jang Su Jin

Department of Nuclear Medicine

The Graduate School

College of Medicine

Seoul National University

Purpose: Nanoparticles as theranostic system are suggested as promising approach in cancer therapy and have been actively investigated worldwide. This study was designed to construct magnetic nanoparticle platform adopting mesoporous silica as safe and efficient coating material for the preservation of magnetic property of metallic core and for the encapsulation of therapeutic materials. For biomedical application, liposomal delivery system of mesoporous silica-coated nanoparticles were adopted. With the particles carrying both chemotherapeutic drug and therapeutic gene, specific targeting of cancer cells and stimulus-sensitive release of therapeutic load were demonstrated. **Methods:** Mesoporous silica shell-coated iron oxide magnetic nanoparticles (MNP@*m*SiO_2) were prepared using a chemical method, and the maintenance of their magnetic and physical properties was examined. To improve their bio-applicability, a liposomal complex system was combined with a MNP@*m*SiO_2 particle (MagLipo). Chemotherapeutic agent,

doxorubicin and the siRNA against Plk1 were loaded in the MagLipo. Active targeting moiety was conjugated onto this nanoparticle and therapeutic efficacy was evaluated. **Results:** The MNP@*m*SiO_2 particles showed remarkable stability and resistance in acidic solution in contrast with bare MNPs. The r_2 value of mesoporous silica shell MNP (MNP@SiO_2) (270 $mM^{-1}\cdot S^{-1}$) was comparable to the bare MNP (286 $mM^{-1}\cdot S^{-1}$), but much higher than the amorphous silica shell MNP (MNP@SiO_2, 70 $mM^{-1}\cdot S^{-1}$). The MagLipo particles were characterized by cryo-TEM analysis as liposomal structures encapsulating between 6 and 8 MNP@mSiO_2 particles. Unlike MNP@*m*SiO_2 particles, MagLipo particles were found to have long-term stability in buffer solution. The MagLipo particles habouring Dox released 40% of Dox within 30 min in pH 4.7 solution. In T_2-*w* phantom study, non-targeting MagLipo treated cells showed similar intensity as the control (nontreated) cells, but the EGFR-MagLipo-treated cells exhibited significantly enhanced black contrast imaging with ≈80% decreasing T2 values. Toxic effect of particle itself was negligible. Furthermore, the MagLipo particles harboring therapeutic drug and gene, were shown to have a dramatic and synergistic therapeutic effect in-vitro. **Conclusions:** The MagLipo particle, as a theranostic material, is promising multifunctional nanovehicle for the specific cancer therapy and imaging at the same time.

Keywords : liposome, magnetic nanoparticle, mesoporous silica, theranostic nanoparticle, pH-sensitive drug delivery
Student Number : 2008-30538